FINITE ELEMENT ANALYSIS OF THIN AND THICK WALLED TUBULAR TEE JOINTS

A. N. GANTAYAT

Engineering Decision Analysis Company, Inc.,
480 California Avenue, Palo Alto, California 94306, U.S.A.

G. H. POWELL

Department of Civil Engineering
University of California, Berkeley, California 94720, U.S.A.

SUMMARY

In this paper a finite element procedure and the associated computer programs for the analysis of thin and thick walled tubular tee joints under a variety of mechanical and thermal loads are described. The analyses were intended particularly for ASA B16.9 standard tees, used in nuclear power plant piping systems. However, the resulting programs are applicable for a much wider range of tee joint geometries.

Intersecting cylinders like piping tees are commonly used components in nuclear reactor systems. Currently both experimental and analytical techniques are available for the analysis of these tees. However, the analytical techniques which primarily use special purpose finite element programs are restricted presently to thin walled tees. For thick walled tees with small radius to thickness ratio, the thin shell elements available in current tee joint programs are unsuitable due to the fact that: (1) flexural shearing deformations which are generally ignored in thin shell analysis may significantly affect the behavior of thick shells; (2) significant strains and stesses may be developed in thickness direction; (3) the strain variation in thickness direction may not be linear. The purpose of this paper is to discuss the development of computer programs which are applicable for the analysis of both thin and thick walled tees.

In order to perform an effective analysis of tee joints by the finite element method, several problems are investigated, including: (1) characteristics of different types of relevant finite elements; (2) procedure for automated generation of finite element data; and (3) the computational efficiency of the computer programs used in the analysis. The basic element considered in this investigation is an eight node isoparametric element proposed originally by Zienkiewicz and Irons (ZIB8). Three different modifications of this element are considered: one modified by the addition of nine incompatible modes (ZIB8R9) one with only three added modes (ZIB8R3), and one with five added modes (ZIB8R5). In order to determine which of the various elements is most suitable for the analysis of tee joints, a number of simple test structures have been studied. These structures were selected to test the performance of the element for the type of behavior to be expected in tee joint configurations. On the basis of these analyses, it was considered that the element ZIB8R9 is most suitable for the analysis of tee joints.

Next, descriptions of three computer programs are presented for: (1) stress analysis under arbitrary mechanical load, (2) transient heat flow analysis, and (3) thermal stress analysis for temperature distributions determined from heat flow analysis. Results of typical analyses applicable to both thin as well as thick walled tees are presented.

It is finally concluded that the developed computer programs are computationally efficient and easy to use for comprehensive analysis of thin and thick walled tubular tee joints under different loading conditions.

1. Introduction

ASA B16.9 tees are commercially available butt welded fittings which normally have a smooth transition between run and branch pipes. Typical sections through the walls of two tees in the crotch region are shown in Fig. 1. It may be observed that although the Schedule 40 joint might qualify as a moderately thin shell, it is doubtful that an analysis based on thin shell assumption will give accurate results for the Schedule 160 joint. Because of unavailability of adequate information in literature which can be applied directly in the development of stress indices for these tees, an extensive series of experimental and analytical investigations were carried out by Oak Ridge National Laboratory. This paper summarizes the research effort undertaken at the University of California at Berkeley under the sponsorship of Oak Ridge National Laboratory, to develop suitable analytical techniques, which may be applied directly for the analysis of ASA B16.9 standard tees, under a variety of mechanical and thermal loads. Although the analytical procedures described in this paper are intended particularly for ASA B16.9 standard tees, the resulting computer programs are applicable to a much wider range of joint geometries with different diameter to thickness ratio.

Based on the analytical studies, three computer programs have been developed for (a) stress analysis of tubular joints under essentially arbitrary mechanical loadings, (b) transient heat flow analysis assuming specified time and location dependent temperature changes on the inner surface and insulated outer surface, and (c) thermal stress analysis for temperature distribution determined by the heat flow analysis.

The finite element method has been selected as the only feasible method of analysis. A number of subproblems have been investigated, in particular (a) characteristic of different finite elements applicable for tubular joint analysis (b) procedure for automated generation of finite element mesh data. Detail discussion of these and other problems are contained in this paper, the computer programs are described and the results of analysis of a number of examples including comparison with experimental results are presented.

2. Finite Element Selection for Tee Joint Analysis

2.1 Candidate Finite Elements

The relative merits of a number of three dimensional elements have been examined by Clough [1], who concluded that the isoparametric hexahedral family of elements originated by Zienkiewicz and Irons [2] are the best available. Accordingly, only elements of this family have been considered for the tubular joint analysis.

The basic hexahedral element considered in this investigation is an 8 node hexahedron of arbitrary shape but with straight edges (ZIB8). The element has three translational degrees of freedom per node and hence have 24 degrees of displacement freedom per element. Fig. 2 shows the global and local coordinates and the corresponding displacements. In order to improve the flexural behavior of this element three different modifications have been considered, one modified by addition of 9 added modes(ZIB8R9), one with only three added modes(ZIB8R3), and one with 5 added modes(ZIB8R5). In addition to these elements, a 20 node hexahedral element with curved edges (ZIB20) is also investigated. The displacement expansion and characteristics of ZIB8 and ZIB20 elements are discussed in reference [1]. The displacement expansions for the ZIB8R9 element are as follows:

$$u = \sum_{i=1}^{8} p_i u_i + \alpha_1 (1 - r^2) + \alpha_2 (1 - s^2) + \alpha_3 (1 - t^2)$$

$$v = \sum_{i=1}^{8} p_i v_i + \beta_1 (1 - r^2) + \beta_2 (1 - s^2) + \beta_3 (1 - t^2) \quad (1)$$

$$w = \sum_{i=1}^{8} p_i w_i + \gamma_1 (1 - r^2) + \gamma_2 (1 - s^2) + \gamma_3 (1 - t^2)$$

in which

$$p_i = \frac{1}{8} (1 + r_o) (1 + s_o) (1 + t_o) \quad (2)$$

and $r_o = rr_i$, $s_o = ss_i$, and $t_o = tt_i$. Subscript i refers to the coordinate values at node $i(\pm 1)$; (u_i, v_i, w_i) are the global displacements at node i; and $(\alpha_i, \beta_i, \gamma_i)_{i=1,2,3}$ are the generalized displacements corresponding to the added incompatible modes of deformation.

The stiffness matrix for the resulting element is of size 33x33. However, when the strain energy within the element is minimized with respect to the α_i, β_i and γ_i, 9 additional equations are obtained, which permit the α_i, β_i, γ_i to be eliminated. The resulting (condensed) stiffness matrix is therefore of size 24x24.

For a shell it would appear to be unnecessary to consider all 9 additional modes of deformation. Instead, it may be sufficient to add modes to permit the element edges to curve in the direction normal to the shell surface, but not to permit them to curve within the shell surface. It is also necessary to include a provision for the normal strain effect. The resulting element will not have isotropic properties.

If it is assumed that the t axis is essentially normal to the shell surface, than the modes added to the displacement, u_t, parallel to this axis are given by

$$u_t = \alpha_1(1 - r^2) + \alpha_2(1 - s^2) + \alpha_3(1 - t^2) \quad (3)$$

in which the first two terms account for bending and the third for the normal strain effect. No additional modes are introduced for the u_r and u_s displacements. The resulting element is identified as ZIB8R3. If d_x, d_y and d_z are the direction cosines of the t axis with respect to the x, y and z axes, respectively, the displacement expansion for this element is

$$u = \sum p_i u_i + \alpha_1 (1-r^2) d_x + \alpha_2 (1-s^2) d_x + \alpha_3 (1-t^2) d_x$$

$$v = \sum p_i v_i + \alpha_1 (1-r^2) d_y + \alpha_2 (1-s^2) d_y + \alpha_3 (1-t^2) d_y \quad (4)$$

$$w = \sum p_i w_i + \alpha_1 (1-r^2) d_z + \alpha_2 (1-s^2) d_z + \alpha_3 (1-t^2) d_z$$

where p_i are as defined for Eq. (2)

The resulting stiffness matrix is of size 27x27. After eliminating the 3 added generalized displacements α_1, α_2, α_3 by static condensation, a stiffness matrix of size 24x24 is obtained.

An element with 5 added modes (ZIB8R5) has also been considered. A weakness of both the ZIB8R9 and ZIB8R3 elements is that the curvatures permitted by the additional modes are constant within the element. Additional freedom to bend can be introduced by adding modes which permit linear variations of curvature, such that the curvature paralled to, say, the r axis remains constant along this axis but may vary linearly in the s direction. The modes added to the u_t displacement are

$$u_t = \alpha_1 (1-r^2)(1+s) + \alpha_2 (1-r^2)(1-s) + \alpha_3 (1-s^2)(1+r) + \alpha_4 (1-s^2)(1-r) + \alpha_5 (1-t^2) \quad (5)$$

For this element a 29x29 stiffness matrix is obtained, which is again condensed to 24x24.

2.2 Comparison of Elements

In order to determine which of the various elements is most suitable for the analysis of tee joints, a number of simple test structures have been studied. These structures were selected to test the performance of the element for the types of behavior to be expected in tee joint configurations. The structures include straight and curved cantilevers, a thin plate, a thin cylindrical shell and a flared axisymmetric shell.

2.2.1 Straight Beam

An indication of the relative bending efficiency of the several solid elements can be obtained from the analysis of a simple symmetrical beam. A beam with the dimensions and finite element subdivision shown in Fig. 3 has been studied. A 10x2x1 mesh was used in the half structure. The results for an applied end moment and an applied end shear are shown in Table 1. It can be seen that the ZIB8 element performs poorly, whereas all other elements give accurate results for both loading conditions.

2.2.2 Curved Beam

One half of the curved beam shown in Fig. 4 has been analyzed to determine the effects of bending when the inner and outer fibers differ in length. Two loading cases have been considered, namely moment and shear as shown. A 10x2x1 mesh was used for the half structure. Results were also computed using the theory of elasticity for a curved beam with a plane stress assumption [3].

The tip displacements and the stresses at the axis of symmetry are compared in Table 2. The ZIB8 element is again seen to perform poorly. However, there are no significant differences among the three modified 8 node elements and ZIB20 element.

2.2.3 Thin Plate

To examine further the bending behavior of the elements, a rectangular plate with uniform load, simple supports on two sides, and clamped and free supports respectively on the remaining two edges (Fig. 5) has been analyzed, for two different ratios of span to thickness, namely 80:1 and 20:1. Three different meshes, namely 2x2x1, 4x4x1 and 8x8x1, were used for one half of the plate (2x2x1 and 4x4x1 only for the ZIB20 element). Numerical results are shown in Table 3.

The results shows the remarkable improvement in bending behavior which is obtained by introducing the incompatible modes. The deflections and stresses are both greatly improved for the modified elements compared to the basic ZIB8 element. A further significant conclusion is that the ZIB8R5 element gives better results than the other modified elements.

2.2.4 Thin Cylindrical Shell

To examine the effectiveness of the modified elements for analyzing thin shells, a cylindrical shell with the geometry, material properties and loading shown in Fig. 6 was analyzed. The shell is supported on diaphragms which allow no displacements in their own planes, but offer no resistance to displacements perpendicular to these planes.

A quarter of the shell was analyzed, using 4x6x1 and 8x12x1 meshes (4x6x1 only for the

ZIB20 element). The deflections at midspan at the crown and edge are compared in Table 4 with results from a thin shell finite element analysis [4] and an "exact" theory [5].

Once again the poor results given by ZIB8 element are evident, and the modified 8 node elements give better results. The ZIB8R5 element is seen to be comparable to the thin shell finite element.

2.2.5 Flared Tube

To investigate the applicability of the modified element for the analysis of both thin and thick shells with geometries similar to that of a tee joint transition, a flared axisymmetric shell, as shown in cross section in Fig. 7, was analyzed, considering internal pressure loading. Because no exact theoretical results are available for comparison, the structure was analyzed using arbitrary thin shell and axisymmetric solid finite element idealizations. Two different radius to thickness ratios, namely 24:1 and 3:1 were considered. For the three dimensional solid and thin shell analyses, only one quarter of the structure was analyzed, taking advantage of symmetry. For the finite element mesh in these cases arc AO (Fig. 7) was divided into 8 elements, length AB was into eight elements, arc BC was into eight elements, and length CD was into four elements. For the three dimensional solid analyses only one layer of elements was provided through the thickness.

For the axisymmetric solid idealization, AB was divided into sixteen elements, BC into sixteen elements and CD into eight elements. Three layers of elements were provided through the wall thickness. This fine mesh was used to ensure an accurate result, which could be assumed to be correct for purposes of comparison. The axisymmetric solid element was that used in the SAP program [6], and contains incompatible modes comparable to those in the ZIB8R9 element.

Results are shown in Fig. 8a for the case R:t = 24:1. The poor performance of the unmodified ZIB8 element in the thin walled configuration is again evident in Fig. 8a. The results for the thin shell and axisymmetric solid elements are seen to agree well, and the results obtained with the modified ZIB8 elements are also accurate.

Results are shown in Fig. 8b for the case R:t = 3:1. For this case, the axisymmetric solid analysis can be expected to be most accurate. The results show that the thin shell element is not accurate for thick shells. The ZIB8 element is again inferior compared to the modified elements, but the ZIB8R3 and ZIB8R9 elements give good results. Of particular interest in these results are the excessively large displacement given by the ZIB8R5 element. This example and the example following show that the supplementary deformation modes used in this element permit excessive shearing deformations. This property is not important for thin shells, in which transverse shearing deformations are negligible, but for thick shells the element gives excessively flexible results.

2.2.6 Deep Cantilever Beam

To investigate the properties of the elements for cases in which shearing deformations are predominate, and hence the consequences of inter-element incompatibility can be expected to be more serious, a cantilever with a span to depth ratio of 1:1.2, subjected to an end shear load, has been analyzed. Four cases with different numbers of elements through the depth have been considered.

The tip deflections, computed at the mid depth, are plotted against the number of element layers in Fig. 9, and compared with the theoretical deflection computed using elasticity theory [7]. It can be seen that the ZIB8R5 element gives excessively large deflections for all cases, and that the ZIB8R9 element substantially overestimates the deflection for the case with two element layers.

2.3 Selection of Element

From the results of the previous section, the following conclusions may be drawn.

(1) The basic 8 node element (ZIB8) gives poor results for the bending of thin plates and shells, and hence is unsuitable for tee joint analysis.

(2) The 20 node element (ZIB20) gives satisfactory results for moderately thick plates and shells. However, the inherent complexity of the element is a disadvantage, so that the application of the element to tee joint analysis is difficult.

(3) The modified 8 node element with five added modes (ZIB8R5) may give displacement results which are significantly in error because of excessive shear deformations in thick shells. However, this is not believed to be a serious disadvantage.

(4) The modified 8 node element with nine added modes (ZIB8R9) may significantly overestimate the deflections for thick shells when two layers of elements are provided through the thickness.

(5) The modified 8 node element with three added modes (ZIB8R3) gives results for plates and shells which are close to those for the ZIB8R9 element, yet avoids the problems of excessive flexibility.

It appears from this investigation that the ZIB8R3, ZIB8R9 or ZIB8R5 elements should all be suitable for the analysis of tee joints. Of these three elements the ZIB8R3 element is more consistant in its performance, whereas the ZIB8R5 element has the most flexible bending characteristics. However, both of these elements have displacement expansions which are anisotropic with respect to the global coordinate system. As a result, the computational procedures for evaluation of the stiffness matrices for these elements are substantially more complex than for the ZIB8R9 element, which has an isotropic displacement expansion. For this reason, it was decided to use the ZIB8R9 element for the tee joint computer programs. This element combines inherent simplicity with the ability to give good results for plates and shells with moderately fine element subdivisions. For a given total number of nodes this element gives results comparable to the 20 node element, but requires less computational effort.

3. Definition of Geometry

3.1 Pentagonal Axes

The subdivision of the joint into finite elements of appropriate size and shape is no less important than the selection of the finite element model. The surface of one quadrant of the tee joint is divided into quadrilateral elements by selecting a control point at the center and drawing lines from this point to the mid point of each boundary line. The location of any point on the joint surface is defined with respect to a pentagonal system of axes A1 through A5 as shown in Fig. 10. Within any one of the five quadrilateral areas into which the surface is divided, a point is identified by the number of mesh subdivisions along each of the two axes adjacent to that quadrilateral. These axes are identified as Axis-1 and Axis-2. Thus, any point on the surface is identified by (i) the number of the quadrilateral in which the node is included (ii) the division number along Axis-1, and (iii) the division number along Axis-2. All of the input and output informations to and from the computer programs are referred to this pentagonal numbering scheme. However, although the nodes are identified by the pentagonal system for input and output, they are renumbered internally by the program to provide a minimum band width.

3.2 Generation Options

The finite element mesh data on each surface of the joint may be specified using different options. In Option 1, the coordinates of all of the nodes in the joint region may be defined for the particular surface being generated by measurements made on the actual joint. In Option 2, the node coordinates may be generated automatically, assuming a mathematical form of the joint surface, and specifying a small amount of data. The specified data in this option should be sufficiently flexible and accurate to accomodate wide variety of joint geometrics. In Option 3, the node coordinates of one surface may be generated from the node coordinates in the other surface (which must have been previously defined) by projecting specified distance through the wall thickness. All these options for defining the finite element mesh are available in the computer programs described in Section 6. Procedure for automatic generation of finite element mesh for an idealized tee joint geometry is discussed in detail in reference [8].

4. Loading Conditions

The loading on the joint may consist of internal pressure in combination with bending moments, torsional moments, axial forces and shear forces at the ends of the run and branch pipes, as shown in Fig. 11. A "basic loading" consists of any one of the load cases 1 through 13 (Fig. 11) applied by itself. Results for additional loading cases, consisting of any specified linear combination of the basic loadings, may also be considered.

Because of the size of the computational problem, it is necessary to take account of the geometric symmetry of the joint about the XY and YZ planes, so that only one quadrant of the joint is analyzed. Hence, because the loading on the joint may be arbitrary, it is necessary to divide the loading into symmetrical and antisymmetrical components and subsequently to combine the results from these component loadings. Thus, each basic loading can be decomposed into one or more "component loadings", each of which is either symmetrical or anti-symmetrical about the XY and YZ planes.

5. Transient Heat Flow and Thermal Stress Analyses of Tee Joints

5.1 General

The determination of the thermal deformations and accompanying stresses resulting from an input of heat flux can be divided into two separate problems, namely (1) the determination of the temperature field and (2) the determination of the deformations and stresses associated with this temperature field. For transient heat flow and thermal stress analyses of a structure as complex as a tee joint, the finite element method is the only feasible method of analysis.

5.2 Heat Flow Analysis

The finite element used for the heat flow analysis is an 8 node hexahedron of Zienkiewicz-Irons isoparametric type, permitting linear temperature variations along all three axes. The assumed temperature field inside the element and details of derivation of element conductivity and heat capacity matrix are given in reference [8].

Two types of boundary condition need to be considered for general heat flow problems, namely specified nodal temperature and specified heat flow into a node. In the tee joint analyses, the temperature (varying with respect to time) is specified at each node on the inner surface of the joint, and the outer surface is assumed to be perfectly insulated, with zero heat flow.

5.3 Thermal Stress Analysis

After the heat flow analysis is completed, the temperatures at all nodes used in the heat flow analysis are known at each time step of the integration procedure. The corresponding thermal stresses can therefore be determined. The procedure would be simple if identical node locations were used for the heat flow and stress analysis problems. In general, however, these nodal locations will not be identical, for the following reason.

In order to obtain accurate values of the temperature gradients through the wall thickness of the tee, it will be necessary to use several element layers within the wall. It will also be usual to use thinner layers near the inner surface than near the outer surface, because larger temperature gradients can be expected at the inner surface.

In contrast, in order to obtain accurate stress values in the thermal stress anlysis, it will be sufficient to use only a small number of element layers, typically one for moderately thin tees, and no more than three for even very thick tees. Also, it will be usual to space the nodes uniformly through the wall thickness.

The computer programs described in Section 6 accounts for these differences in node locations. It is required that the finite element meshes on the inner and outer surfaces of the joint be identical for both the heat flow and thermal stress analyses. However, the locations of the nodes within the wall thickness may be quite different.

6. Computer Programs

The three programs that have been developed are identified as follows:

(1) B16.9TJ/SA - Stress Analysis of B16.9 Tee Joints by the Finite Element Method.

(2) B16.9TJ/THFA - Transient Heat Flow Analysis of B16.9 Tee Joints by the Finite Element Method.

(3) B16.9TJ/TSA - Thermal Stress Analysis of B16.9 Tee Joints by the Finite Element Method.

All three programs use essentially identical specification procedures for the finite element mesh. The programs all use dynamically allocated data storage, so that no program changes are needed for changes in problem size. The two stress analysis programs have almost unlimited capacity and can consider finite element meshes of virtually any degree of fineness. The program for transient heat flow analysis makes use of an in-core equation solver because of the need to carry out the step-by-step analysis. Hence, the size of problems that can be solved depends on the core capacity of the computer being used.

The stress analysis and transient heat flow analysis programs require punched card input. The thermal stress analysis program obtains the bulk of its data from a tape created during the heat flow analysis and requires only a small amount of control information to be input on cards.

7. Examples

7.1 Thin Walled Tee

To demonstrate the range of applicability of the program B16.9TJ/SA, a thin walled cylinder connection has been analyzed. This example has previously been analyzed using a thin shell finite element idealization (9). The dimensions of the joint are shown in Fig. 12.

Two loading cases, namely internal pressure and in-plane moment on the branch, have been considered.

The inside and outside surface meshes were both generated directly, assuming a very small (0.01 inch) fillet radius. Fig. 13 shows the finite element mesh for the outer surface. It should be noted that a very fine mesh subdivision is necessary near the transition, because of the high stress gradients in this region. A mesh which expands both circumferentially and longitudinally has been used to reduce the total number of nodes and elements.

The computed surface stresses are compared with experimental values in Fig. 14a and 14b. The 0° and 180° lines and the longitudinal and transverse directions are as defined in Fig. 15.

It can be seen that the theoretical and experimental values compare favorably, demonstrating that the computer program is applicable to thin cylinder connections as well as forged tees.

7.2 B16.9 Tees

7.2.1 Finite Element Meshes

Three tees, designated as T8-Sch 40; T6-Sch 80 and T7-Sch 160 have been analyzed using the program B16.9TJ/SA, for 13 load cases each. The results for three of these cases, namely internal pressure, in-plane moment on the branch, and out-of-plane moment on the branch, have been compared with experimental results obtained at Southwest Research Insitute (10).

The plot of the finite element meshes for the joints are shown in Figures 16a through 16d.

7.2.2 Results

The computed stresses for the T8-Sch 40 joint are compared with the experimental results in Fig. 17. The agreement is seen to be close, with the generated and measured meshes giving comparable results. The best agreement between the experimental and finite element results is obtained for out-of-plane moment, and the worst agreement for in-plane moment.

The computed and measured stresses are compared for the T6-Sch 80 joint in Fig. 18. In this case the agreement is not as close as for the T8-Sch 40 joint. In particular, poor agreement is obtained along the 0° line on the inside surface for pressure load and along the 90° line on the inside surface for out-of-plane moment.

8. Summary and Conclusions

8.1 Summary

On the basis of numerical results obtained for several example structures, it has been concluded that modified isoparametric 8 node hexahedral elements are most suitable for analysis of the tee joints. Of the several modified elements considered, that with 3 added incompatible modes (ZIB8R3) appeared to be most consistent in performance, whereas that with 5 added modes (ZIB8R5) had the most flexible bending characteristics. Nevertheless, for reason of computational convenience the element with 9 added modes (ZIB8R9) was selected for the tee joint computer programs.

Because of the size of the problem it is necessary to take advantage of symmetry of the joint about two planes, and to analyze only one quadrant of any complete joint. The loads must therefore be subdivided into symmetrical and antisymmetrical components and the results for these component loadings ultimately superimposed. The operations are carried out automatically within the computer programs.

Various options may be used to define the corresponding finite element meshes on the outer and inner surfaces of the joint. Using one such option it is possible to generate automatically the finite element mesh on a surface by making use of a simplified concept of the joint geometry which requires only a very limited amount of directly measured data as input information.

A procedure for carrying out transient heat flow analyses and corresponding thermal stress analyses for a tee with specified time and space dependent inside surface temperatures and perfectly insulated outside surface has been developed. For these two analyses it may be necessary to provide different numbers of layers of elements through the wall thickness. This has been taken into account in the computer programs.

The three computer programs which have been developed form an integral group, with similar structural idealization and data input procedures. All programs are computationally efficient, and can be applied to finite element meshes of virtually any degree of refinement without program changes.

Stress analysis of a thin walled tee and of schedule 40, 80 and 160 B16.9 tees have been carried out, and the results compared with experimental values.

8.2 Conclusions

From the analysis of the thin walled tee it can be concluded that the results obtained by using the program B16.9TJ/SA compare favorably with experimental values. However, it is necessary to provide a fine mesh subdivision near the transition because of the high stress gradients in this region.

As illustrated, the results obtained for T8-Sch 40 and T6-Sch 80 tees compare reasonably well with the experimental values.

References

[1] CLOUGH, R.W., "Comparison of Three Dimensional Finite Elements", Proceedings, Symposium on Application of Finite Element Method in Civil Engineering, Vanderbilt University, November 1969.

[2] IRONS, B.M., ZIENKIEWICZ, O.C., "The ISO Parametric Element System - A New Concept in Finite Element Analysis", Proceedings, Conference on Recent Advances in Stress Analysis, Royal Aeronautical Society, London, England 1968.

[3] TIMOSHENICO & GOODIER, "Theory of Elasticity", Second Edition, McGraw Hill Book Company, pp 250-253.

[4] JOHNSON, C.P., "The Analysis of Thin Shells by a Finite Element Procedure", SESM Laboratory, Report No. 67-22, University of California, Berkeley, September 1967.

[5] SCORDELIS, A.C., LO, K.S., "Computer Analysis of Cylindrical Shells", Journal of American Concrete Institute Proceedings, V. 61, N. 5, 1964.

[6] WILSON, E.L., "SAP-A General Purpose Structural Analysis Program", SESM Laboratory, Report No. 70-20, University of California, Berkeley, September 1970.

[7] FELIPPA, C.A., "Refined Finite Element Analysis of Linear and Nonlinear Two Dimensional Structures", SESM Laboratory, Report No. 66-22, University of California, Berkeley, December 1966.

[8] GANTAYAT, A.N., POWELL, G.H., "Stress Analysis of Tee Joints by the Finite Element Method", SESM Laboratory, Report No. 7, University of California, Berkeley, 1972.

[9] GRESTE, O., "Finite Element Analysis of Tubular K Joints", SESM Laboratory, Report No. 70-11, University of California, Berkeley, June 1970.

[10] GRIGORY, S.C., DEEL, G.W., "Experimental Stress Analysis and Fatigue Test of ASA Standard B16.9 Tees", Quarterly Report No. 4, SWRI Project No. 03-2567, Southwest Research Institute, Houston.

TABLE 1 RESULTS FOR STRAIGHT CANTILEVER

Deflections and Normal Stresses				
Element Type	Moment Load		Shear Load	
	Deflection at Y=10, Z=0.	σ_y stress at y=4, Z=1	Deflection at y=10, Z=0.	σ_y stress at y=4, Z=1
ZIB8	89.01	2800.00	91.49	2519.90
ZIB8R9	exact	exact	102.63	2699.98
ZIB8R3	exact	exact	102.61	2699.88
ZIB8R5	exact	exact	102.68	2699.98
ZIB20	exact	exact	102.85	2699.40
Theory	100.00	3000.00	103.00	2700.00

TABLE 2 RESULTS FOR CURVED CANTILEVER

Results for Moment Load			
Element Type	Radial Displacement at Tip ($\theta=90^0$)	Normal Stress at Centerline ($\theta=0^0$)	
		Inner Fibre	Outer Fibre
ZIB8	-155.72	-2781.04	2194.48
ZIB8R9	-198.39	-3175.22	2811.16
ZIB8R3	-198.39	-3174.44	2811.98
ZIB8R5	-198.63	-3178.29	2816.35
ZIB20	-195.71	-3115.26	2738.82
Theory	-199.35	-3215.15	2813.02
RESULTS FOR SHEAR LOAD			
Element Type	Radial Displacement at Tip ($\theta=90^0$)	Normal Stress at Centerline ($\theta=0^0$)	
		Inner Fibre	Outer Fibre
ZIB8	-184.52	-4285.47	3125.45
ZIB8R9	-234.61	-4878.33	4048.54
ZIB8R3	-234.60	-4871.41	4044.25
ZIB8R5	-235.83	-4876.88	4051.84
ZIB20	-232.11	-4870.23	4031.62
Theory	-237.02	-4979.95	4074.50

TABLE 3 RESULTS FOR PLATE WITH VARIOUS BOUNDARY CONDITIONS

		Displacement Coefficient $\alpha x10^4$			Stress Coefficient $\beta x10^4$		
	Thin Plate Theory	-582			7032		
$\frac{L}{h}$	Element	2x2x1	4x4x1	8x8x1	2x2x1	4x4x1	8x8x1
80	ZIB8	-2	-8	-29	30	125	476
	ZIB8R9	-28	-256	-542	415	3640	6960
	ZIB8R3	-28	-256	-542	415	3640	6960
	ZIB8R5	-229	-524	-580	1770	6760	7050
	ZIB20	—	-352	-556	—	3960	7090
20	ZIB8	-31	-101	-256	450	1620	3980
	ZIB8R9	-265	-550	-587	3840	7350	7351
	ZIB8R3	-265	-550	-587	3840	7350	7351
	ZIB8R5	-508	-578	-589	6120	7200	7250
	ZIB20	—	-513	-564	—	5970	6980

TABLE 4 RESULTS FOR CYLINDRICAL SHELL WITH FREE EDGE

Element Type	Vertical displacement at mid span (inches)			
	at crown		at free edge	
	4x6x1 mesh	8x12x1 mesh	4x6x1 mesh	8x12x1 mesh
ZIB8	-0.2209	-0.2587	-0.2676	-0.3420
ZIB8R9	0.1890	0.5115	-2.3531	-3.5300
ZIB8R3	0.1889	0.5112	-2.3528	-3.5301
ZIB8R5	0.4778	0.5257	-3.4536	-3.5800
ZIB20	—	0.3501	—	-2.9518
Thin shell finite element	0.5174	0.5469	-3.6156	-3.6626
Thin shell theory	0.552		-3.6960	

F .1/1*

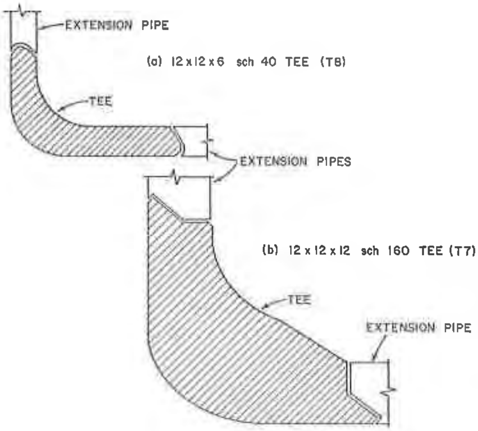

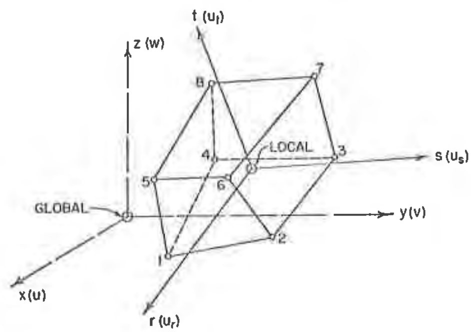

FIG. 1 WALL SECTION IN CROTCH REGION FOR TYPICAL JOINTS

FIG. 2 COORDINATE SYSTEM FOR ZIB8 ELEMENTS

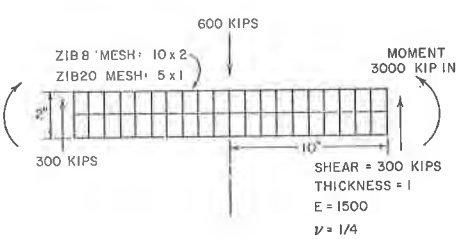

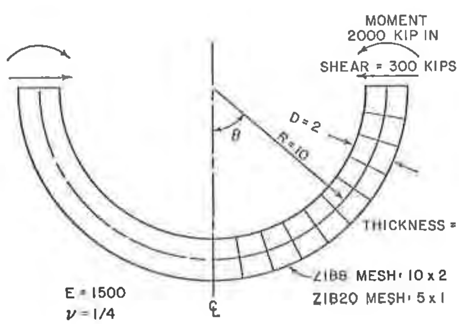

FIG. 3 STRAIGHT BEAM

FIG. 4 CURVED BEAM

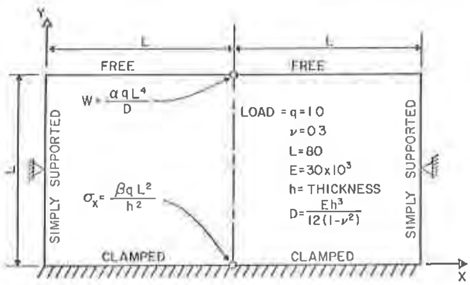

FIG. 5 PLATE WITH VARIOUS BOUNDARY CONDITIONS

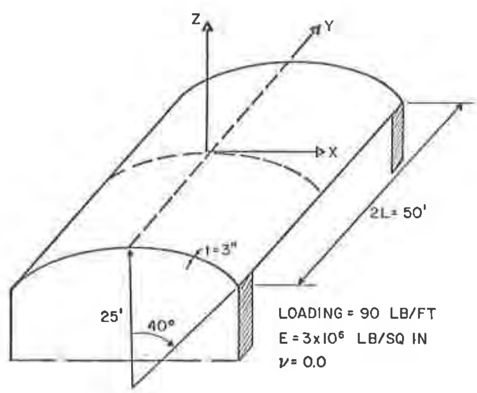

FIG. 6 CYLINDRICAL SHELL WITH FREE EDGE

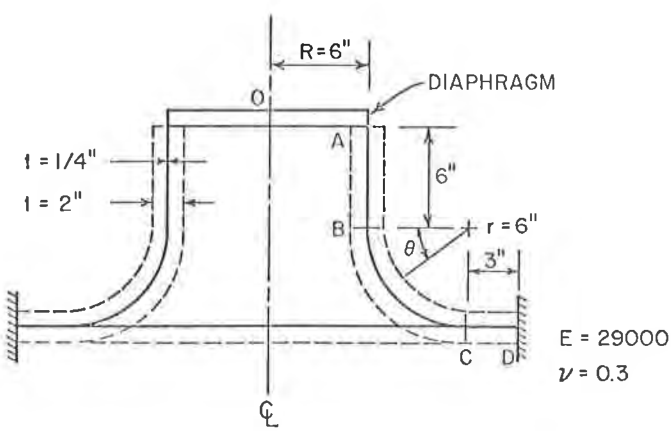

FIG. 7 DIMENSIONS OF FLARED TUBE

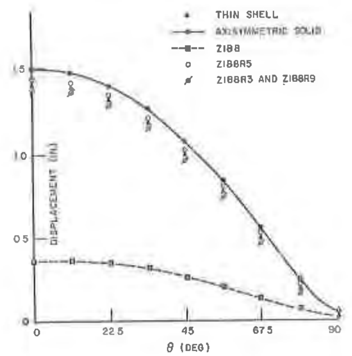

FIG. 8a FLARED TUBE UNDER INTERNAL PRESSURE, R/t = 24

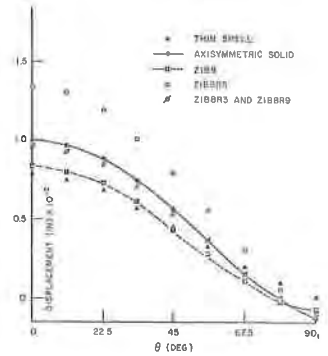

FIG. 8b FLARED TUBE UNDER INTERNAL PRESSURE, R/t = 3

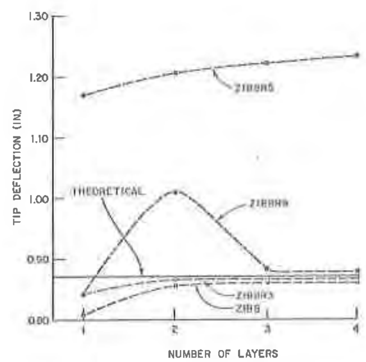

FIG. 9 DEEP CANTILEVER-EFFECT OF NUMBER OF ELEMENT LAYERS

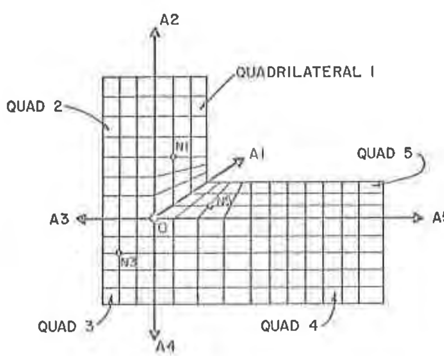

FIG. 10 PENTAGONAL SYSTEM

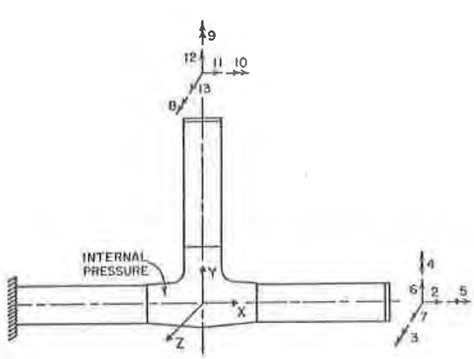

FIG. 11 BASIC LOADINGS

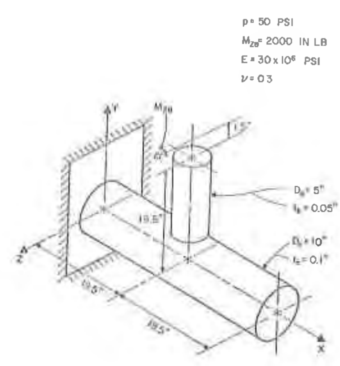

FIG. 12 THIN WALLED TEE

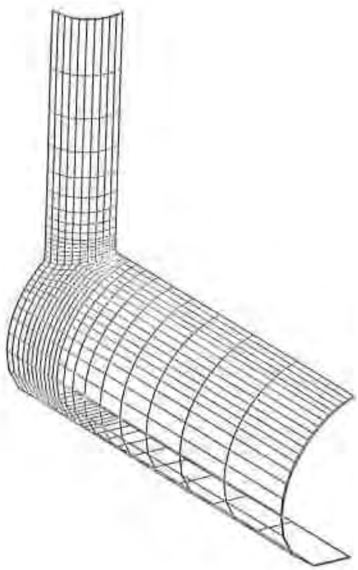

FIG. 13 FINITE ELEMENT MESH. THIN WALLED TEE

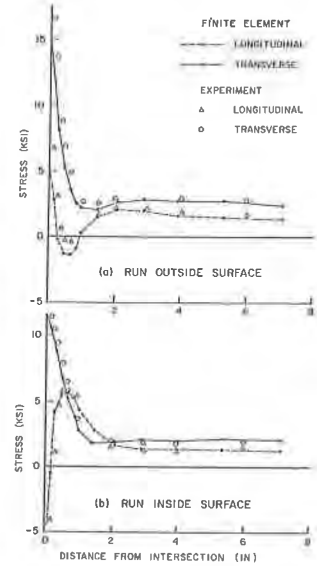

FIG. 14 THIN WALLED TEE. INTERNAL PRESSURE. 0° LINE. STRESSES IN RUN

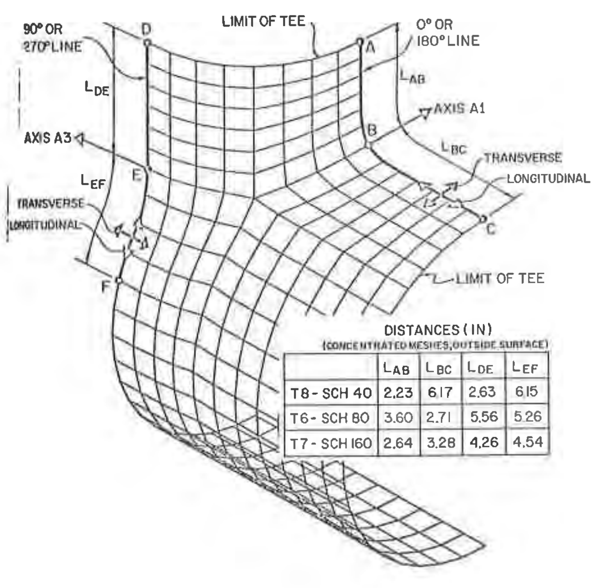

	L_{AB}	L_{BC}	L_{DE}	L_{EF}
T8 - SCH 40	2.23	6.17	2.63	6.15
T6 - SCH 80	3.60	2.71	5.56	5.26
T7 - SCH 160	2.64	3.28	4.26	4.54

FIG. 15 REFERENCE POINTS FOR STRESS VARIATIONS

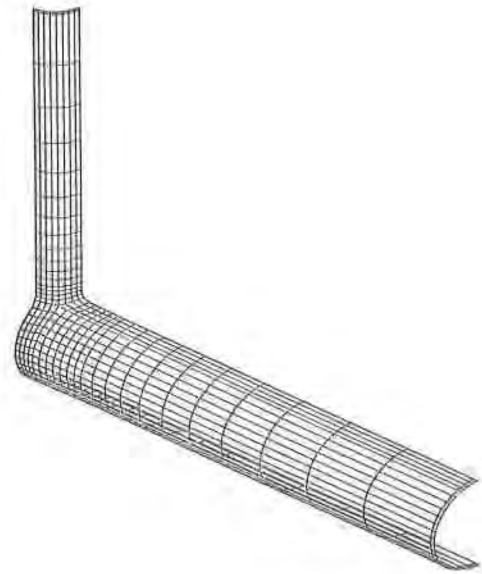

FIG. 16a T8-SCH 40 TEE. GENERATED OUTSIDE MESH

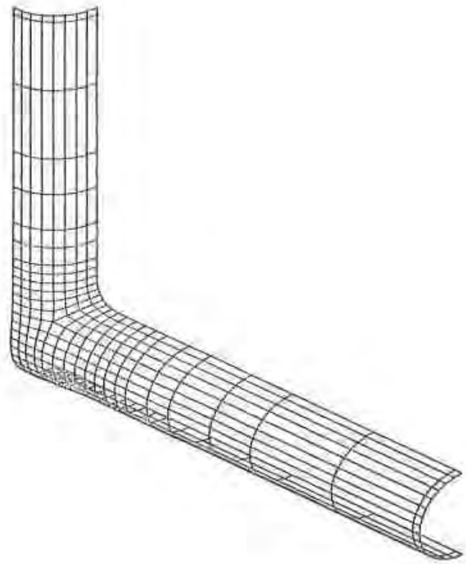

FIG. 16b T6-SCH 80 TEE. MEASURED OUTSIDE MESH

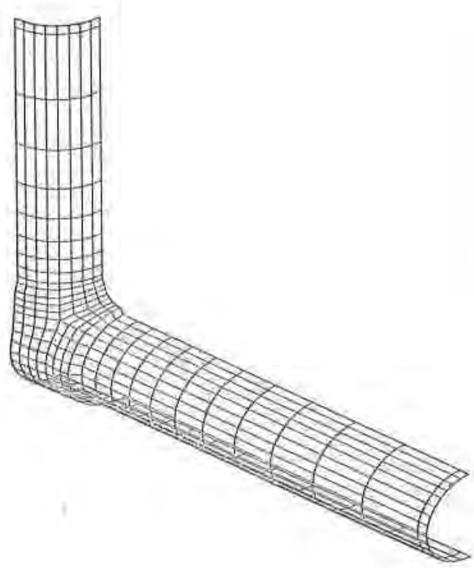

FIG. 16c T7-SCH 160 TEE. GENERATED OUTSIDE MESH

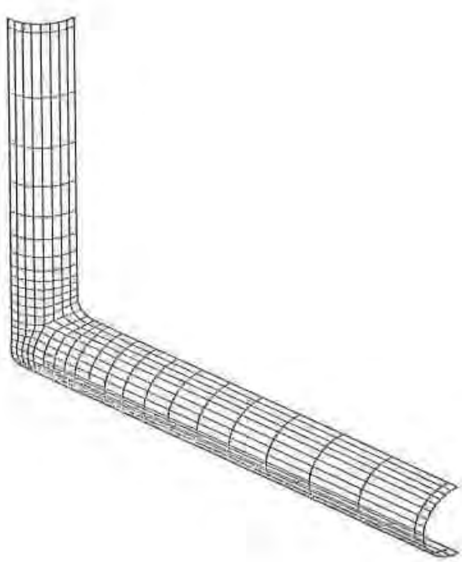

FIG. 16d T7-SCH 160 TEE. GENERATED INSIDE MESH

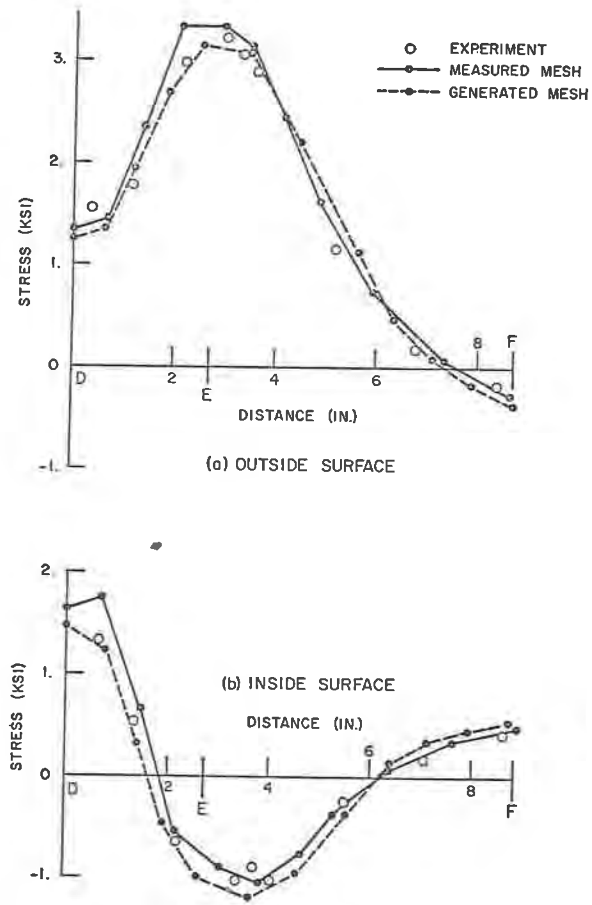

FIG. 17 T8-SCH 40. LONGITUDINAL STRESSES OUT-OF-PLANE MOMENT. 270° LINE

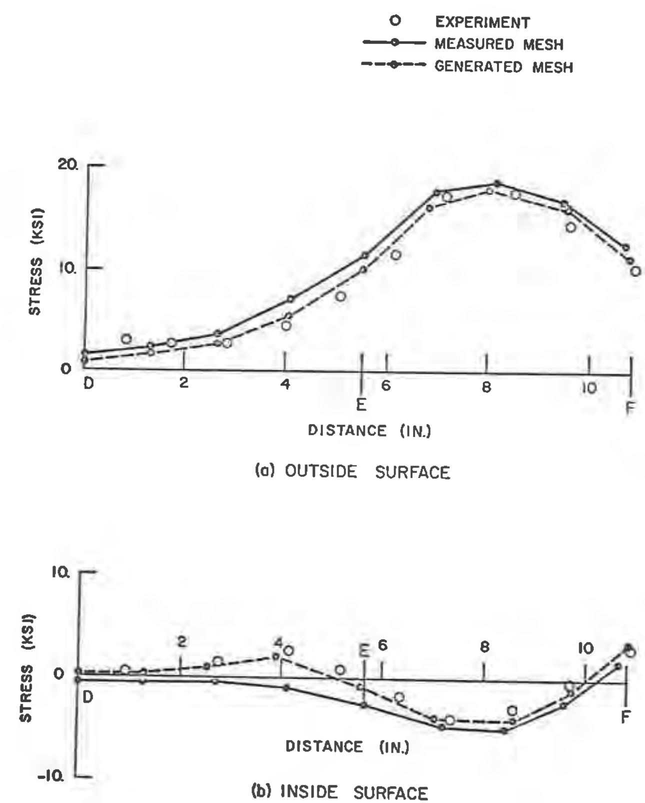

FIG. 18 T6-SCH 80. LONGITUDINAL STRESSES INTERNAL PRESSURE. 90° LINE

F 1/1*